Supporting information for

The Electrostatic Screening-Length in Concentrated Salt Solutions

Prudhvidhar Gaddam[†] and William Ducker*

Department of Chemical Engineering and Center for Soft Matter and Biological Physics, Virginia Tech, Blacksburg, VA 24061, USA.

*For correspondence: wducker@vt.edu

Table S1. Refractive indices for concentrated salt solutions

Salt Type	Salt concentration (mol/L)	Refractive index λ = 445 nm	λ = 470 nm	λ = 525 nm
LiCl	0.5	1.3363	1.3374	1.3363
	2.5	1.3527	1.3529	1.3529
	4	1.3645	1.3643	1.3643
	5.5	1.3757	1.3758	1.3758
	7	1.3854	1.3851	1.3850
	10	1.4055	1.4052	1.4052
CsCl	0.5	1.3429	1.3428	1.3412
	2.5	1.3653	1.3652	1.3644
	4	1.3821	1.3820	1.3818
	5.5	1.3991	1.3990	1.3990
NaCl	0.5	1.3463	1.3447	1.3484
	2.5	1.3587	1.3592	1.3596
	4	1.3680	1.3678	1.3679
	5.5	1.3797	1.3795	1.3796

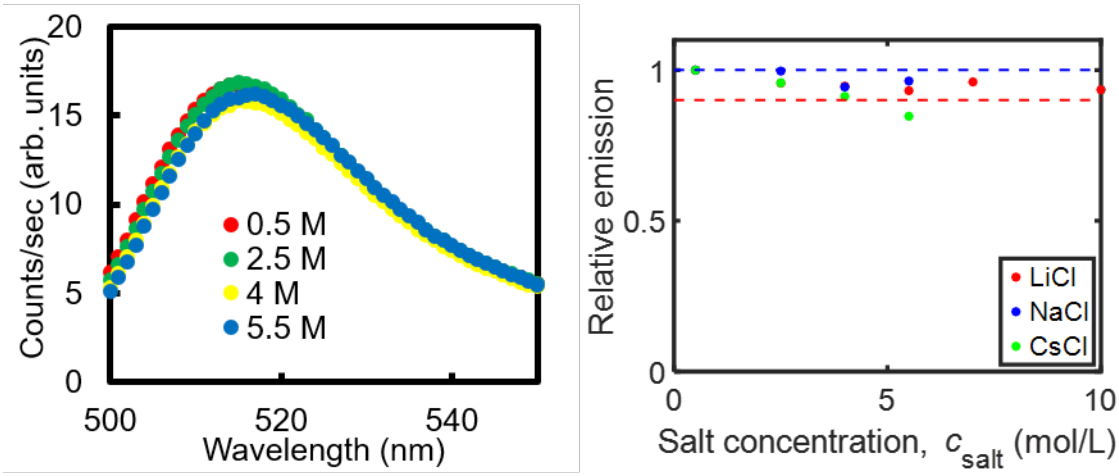

Figure S1. Left: Fluorescence emission of 15 µM aqueous fluorescein solutions for various NaCl salt concentrations. The measured range is from 500 to 550 nm to match the range of the emission filter (550±25 nm) used when measuring the surface excess. Even very large concentrations of salt have a small effect on the spectrum. Fluorescence emission was measured with a Horiba FluoroMax fluorimeter with 475 nm excitation. Right: Relative emission of a 15 µM solution of fluorescein solutions for the different salt types and salt concentrations tested in this work. We define relative emission as:

$$\frac{\text{intergral of spectrum for metal chloride solution}}{\text{integral of spectrum for same fluorescein concentration and 0.5 M metal chloride}}$$

The majority of the data has a relative emission of 1 and 0.9 as indicated by the dashed lines. The exception is 5.5 M CsCl, which is 16% less than that of a reference 0.5 M CsCl solution. Since the fluorescence emission of fluorescein solutions is weakly affected by Li^+ and Na^+ concentration, then:

(a) We are able to use the 0.5 M solution to calibrate the intensity-amount relationship.
(b) We consider it very unlikely that concentrated salt affects dissociation of fluorescein. The fluorescence spectrum of fluorescein is strongly affected by the degree of dissociation of fluorescein.[1]

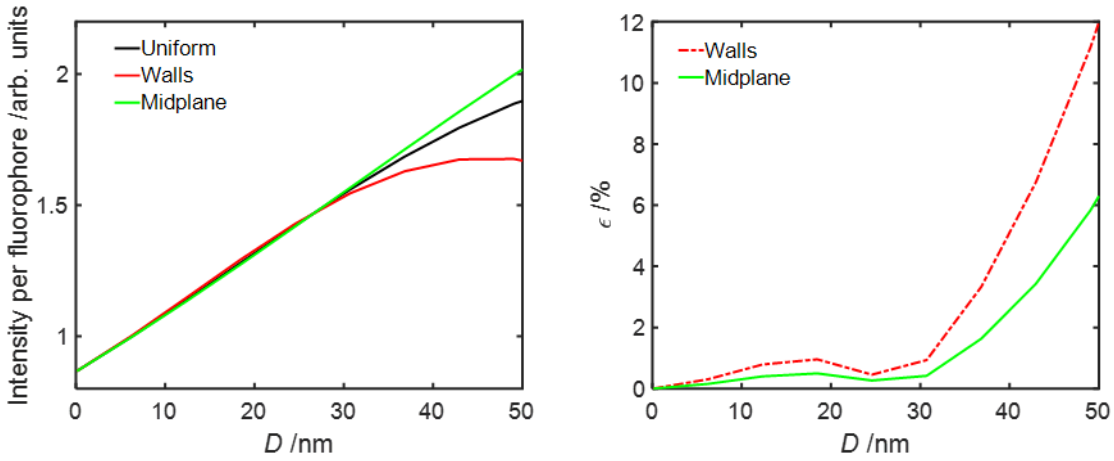

Figure S2. Optical modelling showing the effect of molecular distribution on fluorescence emission. These plots show how the emission is expected to vary for three different *z*-distributions of molecules: uniform, all molecules at the walls (*z*=-*D*/2 and *z*=*D*/2), or all molecules at the midplane (*z*=0). Differences arise because of optical interference in the optical excitation.

Left: Intensity per fluorophore, calculated using the optical model from our earlier publication[2] using an oxide thickness of 41 nm and a fluorescein solution of refractive index, *n* = 1.41, for three examples of fluorophore distribution: uniform, all molecules at the walls (*z*=-*D*/2 and *z*=*D*/2), or all molecules at the midplane (*z*=0). At *D* > 30 nm there is a divergence of the emission from the three different molecular distributions.

Right: Calculated error as a result of assuming that the distribution is uniform when the molecules are either all at the surface or all at the midplane. $\epsilon = \frac{I_{\text{Walls or Midplane}}}{I_{\text{Uniform}}} \times 100\%$. For example, at *D* = 50 nm, if the all fluorophores were all at the walls, our assumption that the distribution were uniform would result in an underestimation of the number of fluorophores by ≈12%. In order to limit this error from dominating our surface excess results, the paper only displays results in the range 0–30 nm. The uncertainty due to the distribution is seen to be relatively low (< 2%) in this range.

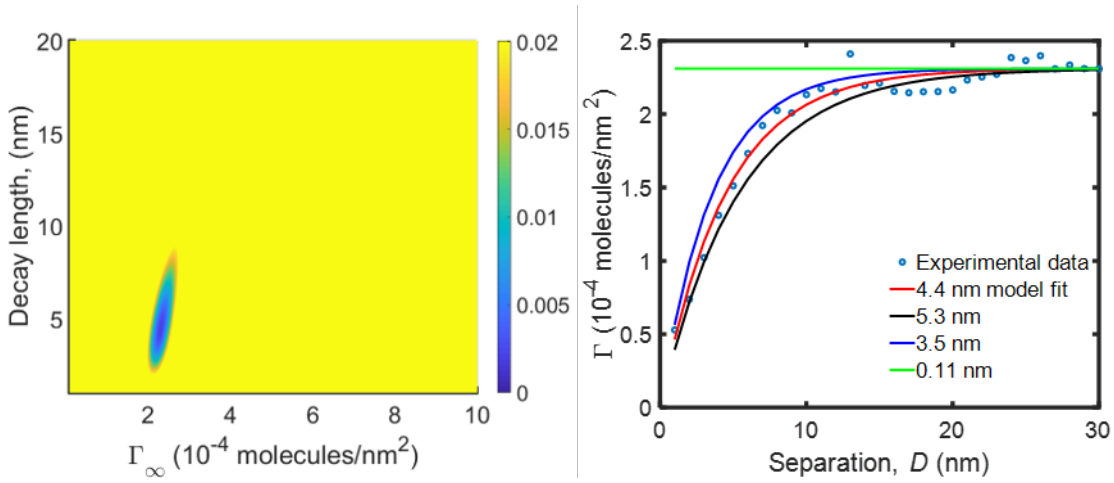

Figure S3. Uncertainty in the fit of the Decay-length from the empirical equation (Eq. 4)

Left: Error heat map showing the least-squared sum of deviations between experimental data from one chip (4 M LiCl) and the surface excess obtained from the empirical model for the surface excess (Eq. 4) for a matrix of terminal surface excesses (Γ_∞) and decay-lengths (κ_E^{-1}). The fit was done over the range 0–30 nm. Color indicates extent of deviation. The minimum error sum is about 0.002 (blue) corresponding to a terminal surface excess of Γ_∞ = 2.31 molecules/nm^2 and κ_E^{-1} = 4.4 nm. The heat map shows that there is a unique minimum, and that the minimum well is narrower in the terminal surface excess than the decay-length.

Right: Experimental data from one chip (4 M LiCl) and four different curves calculated using Eq. 4: red is the best fit of the decay length, the black line was calculated using 120% of the best fit decay length, the blue line 80% of the best fit decay length, and green used a fixed decay length equal to the Debye-length for a 4 M LiCl solution (0.11 nm). Clearly the Debye-length does not allow a good fit.

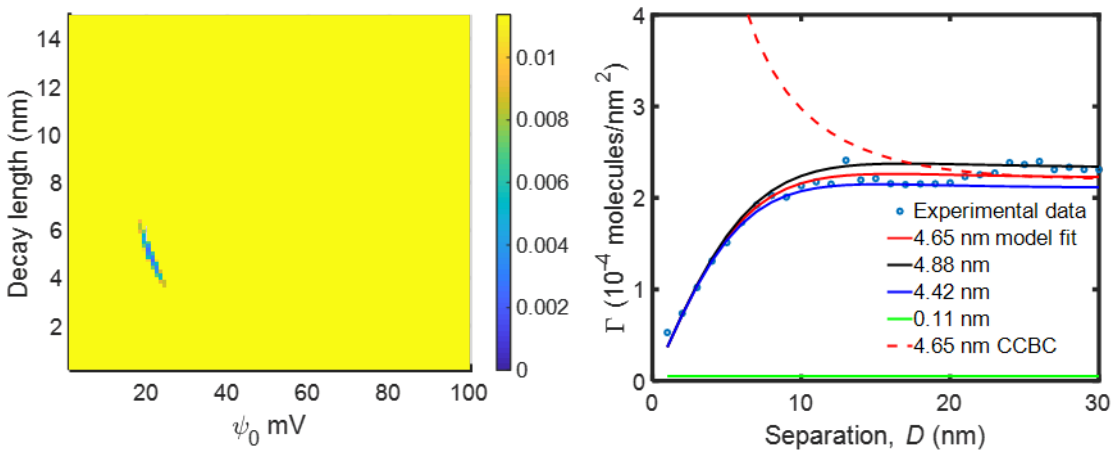

Figure S4. Uncertainty in the fit of the Decay-length from the modified Poisson-Boltzmann equation.

Left: Error heat map showing the least-squared sum of deviations between experimental data from one chip (4 M LiCl) and the surface excess obtained from the analytic low-potential solution of the Poisson-Boltzmann equation (Eq. 6) for a matrix of surface potentials and decay-lengths. The fit was done over the range 0–30 nm. Color indicates extent of deviation. The minimum error sum is about 0.002 (blue) corresponding to a surface potential of ψ_0 = 21 mV and κ_F^{-1} = 4.65 nm. The heat map shows that there is a unique minimum, and that the minimum well is narrow in potential but relatively broad in decay-length, stretching from about 4–6 nm.

Right: Experimental data from one chip (4 M LiCl) and four different theoretical curves using the best fit potential from Eq. 6, but different decay lengths: red is the best fit of the decay length, the black line was calculated using 95% of the best fit decay length, the blue line 105% of the best fit decay length, and green line is the best fit when the decay length was fixed as the Debye-length for a 4 M LiCl solution (0.11 nm). Clearly the Debye-length does not provide a good fit, and the uncertainty of the decay length in the fit is small – a fraction of a nm. The dashed red line is the exact numerical solution with a constant charge boundary condition (CCBC). For this calculation we used the same surface charge density at infinite separation and decay length that were obtained for the best fit at constant potential, σ_0= 0.000954 charges/nm^2. Clearly the constant charge boundary condition is not even qualitatively consistent with the measured data because the measured density of fluorescein does not rise as the separation decreases. According to PB theory, the surface excess is more sensitive to surface charge regulation than the surface forces.

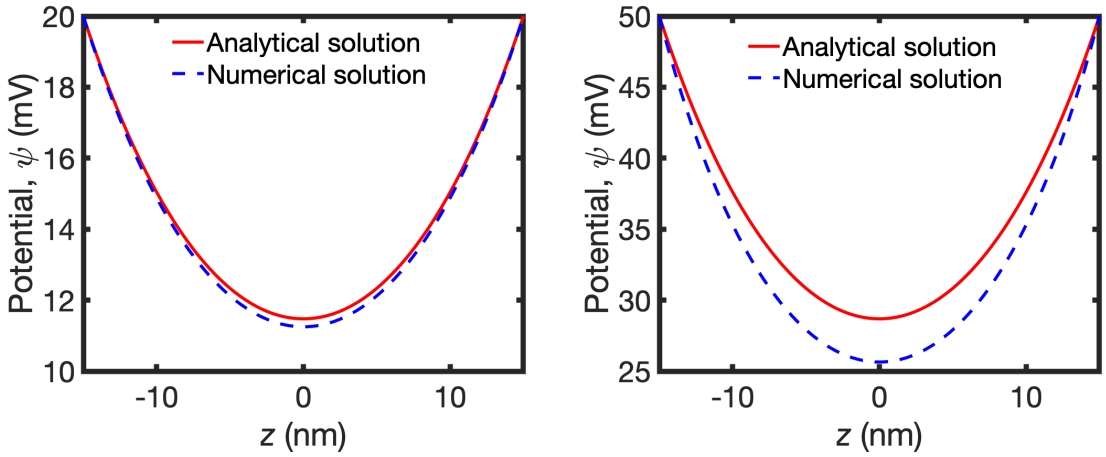

Figure S6. Comparison of exact numerical solution and low-potential analytical solution of the modified Poisson-Boltzmann equation for the constant potential boundary condition.

Left: Comparison of analytical solution for the low-potential approximation and exact numerical solution of the Poisson-Boltzmann equation for a surface potential, ψ_0 of 20 mV, a decay length κ^{-1} of 13 nm and total film thickness, *D* = 30 nm.

Right: Potential plot for the same decay length and total film thickness, but for a greater surface potential, ψ_0 of 50 mV. The plots show that low potential approximation has an increasing error as the potential grows, as expected. This error translates into an error in the Decay-length used to fit our surface excess measurements. For ψ_0 < 25 mV, the error in Decay length was <2 %, for 10 M LiCl (ψ_0 = 45 mV) the error was 10%.

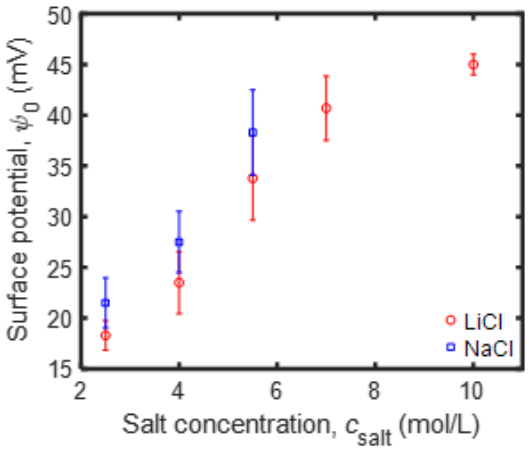

Figure S7. Fitted surface potentials as a function of salt concentration for LiCl and NaCl. The error bars represent standard error for the fitted potential from 4 experimental repeats.

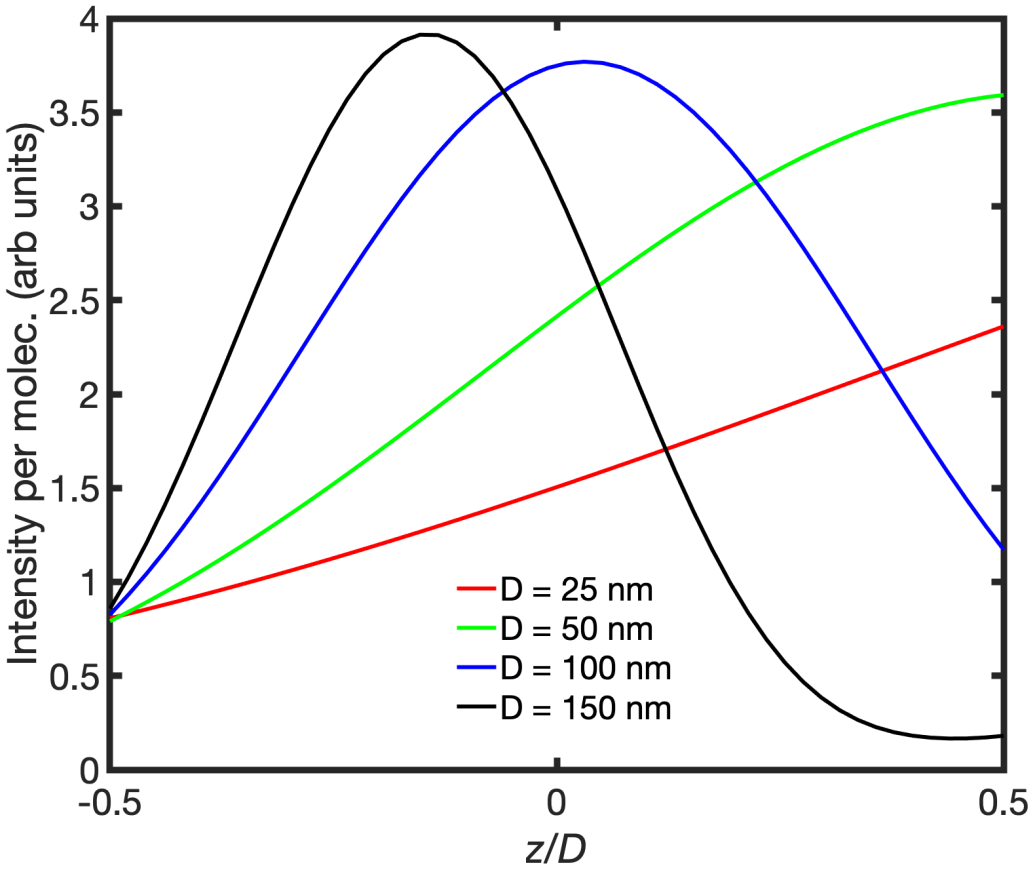

Figure S8. Optical model showing intensity per molecule as a function of position in the film for various aqueous film thicknesses and a 41 nm oxide film. z/D = 0 is the midplane, z/D = –0.5 is the silicon-oxide–solution, and z/D = 0.5 is the glass–solution interface. Although the overall shape of the curves is similar when plotted on a z-axis, the relative contribution from different parts of the film varies greatly. For a 25 nm film, the emission intensity for a molecule at the glass–solution interface is about 3× greater than for a molecule at the silicon-oxide –solution interface. For a 150 nm thick film, the roles are reversed: the intensity is about 4 × greater at the silicon-oxide–water interface.

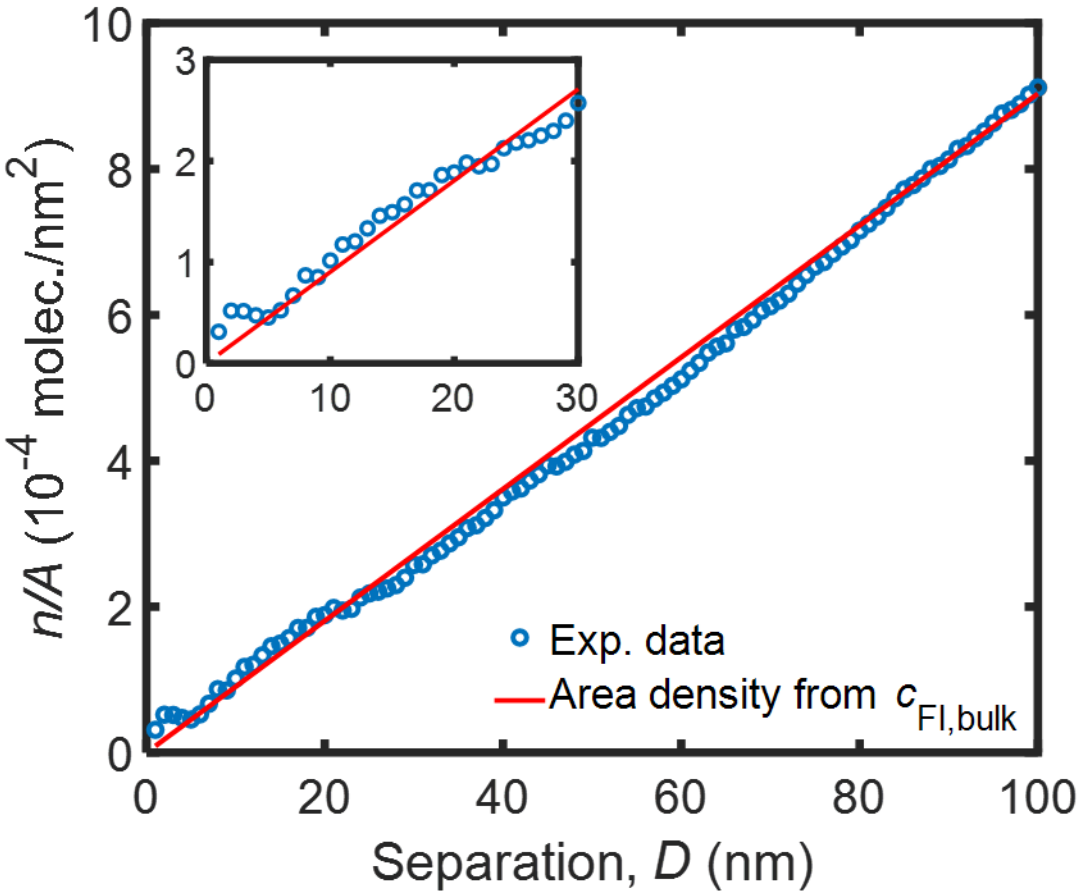

Figure S9. The number of fluorescein molecules per unit area between the two solid–liquid interfaces. The red line assumes that the concentration in the film is the bulk concentration for all thicknesses of film. The red line is the bulk concentration (determined from the mass, molecular mass and volume of the solution) multiplied by the thickness of the film. The blue circles are intensity measurements divided by a single calibration constant, the intensity per molecule, obtained from the fit in Fig 10. The close agreement between the model and the experiment in the region 0–20 nm shows that bulk solution extends all the way to the crack tip: there is no surface excess or no long-range decay in 0.5 M LiCl solution, which is a stark contrast to results in the more concentrated solutions. The inset shows more detail of the thin film region, D = 0 – 30 nm.

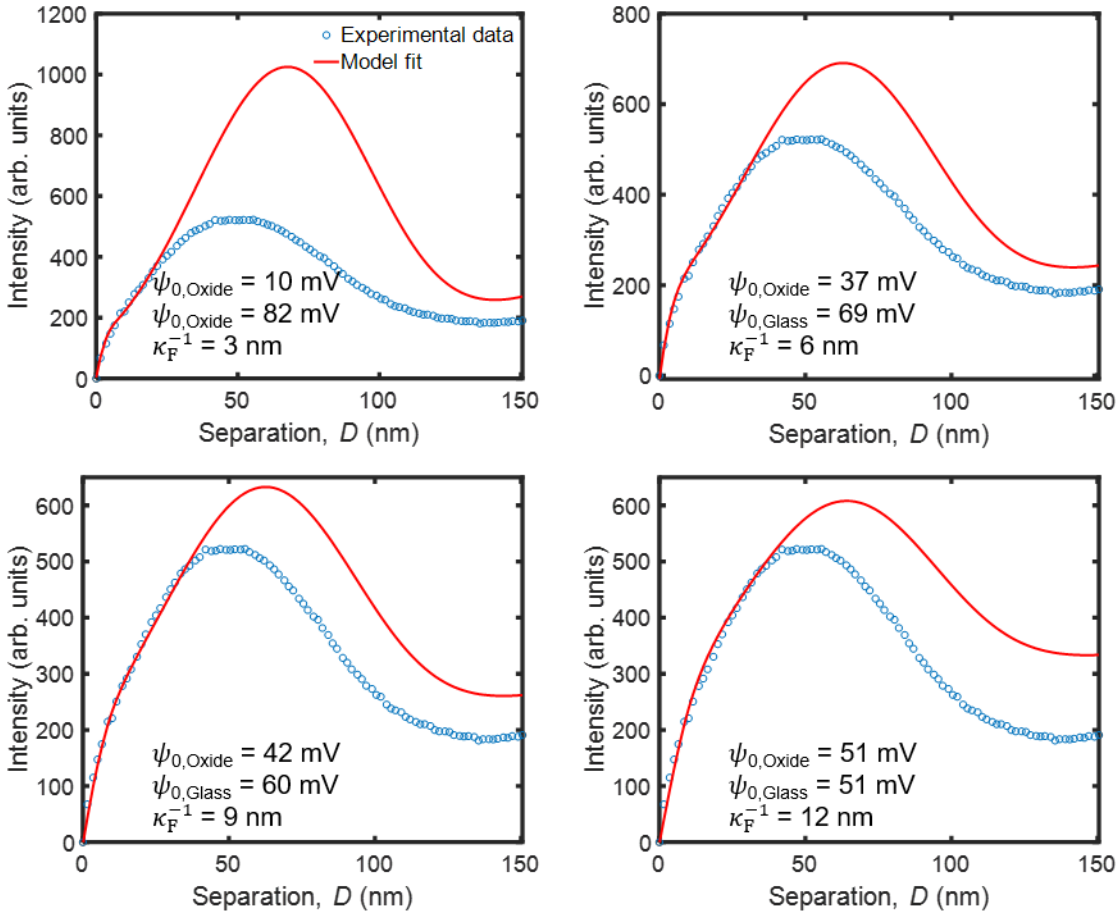

Figure S10. Effect of asymmetry on the fit of the decay length. The glass contains 13% boron, 4% sodium and 2% aluminum substitution for silicon, which could result in a difference in charging behavior between the glass–solution interface and the silicon-oxide–solution interface. In this figure, we have examined how a different potential on each surface affects the PB fit to the data for the 10 M LiCl experiment over the range of D = 0–30 nm. These fits are for the exact numerical solution to PB equation, assuming that the interface potential is independent of *D*. These are significant assumptions. Each figure shows the best fit for a particular decay-length that is indicated. The fits are reasonable over 0–30 nm for all the decay lengths. However, an increasing degree of asymmetry in potential is required for a lower decay length. We consider a large asymmetry to be unlikely. In addition, for the 3 and 6 nm decay lengths, the fit becomes qualitatively more unreasonable for larger separations. The best fit for the asymmetric potentials (decay = 9 nm) is better than the best for symmetric potentials (decay = 12 nm). This is necessarily true because there is an additional fit parameter: the degree of asymmetry.

Summary: In this manuscript we have assumed that the surface potentials are symmetric, but the analysis above suggests that the data could be better fit with an asymmetric potential. The conclusions of the paper would still be retained by allowing asymmetry of the potentials, but it is not clear that the additional degree of freedom in the analysis is justified for a model that already has significant

assumptions (functional form of solution to PB equation, constant potential, decay length independent of confinement)

References

1. Martin, M. M.; Lindqvist, L. J., The pH dependence of fluorescein fluorescence. Journal of Luminescence, **1975,** *10* (6), 381-390.
2. Gaddam, P.; Grayson, R.; Ducker, W., A., Adsorption at Confined Interfaces. *Langmuir* **2018,** *34* (36), 10469-10479.